DOMINATING FACTORS IN SLURRY TRANSPORT IN INCLINED PIPES

Sape A. Miedema[1], F. Wang[2], G. Hong[3] & X. Chen[4]

ABSTRACT

In deep sea mining, the valuable materials will often be transported to the surface by means of slurry transport through pipelines, using centrifugal pumps to generate the pressure. The slurry transport pipeline has vertical, but also inclined trajectories. It is thus of interest what are the dominating factors in slurry transport in inclined pipes. Here this is investigated for Newtonian settling slurries. Experiments to investigate the dominating factors in slurry transport in inclined pipes were carried out in the CCCC National Engineering Research Center of Dredging Technology and Equipment, Shanghai, China. These experiments were carried out in a D_p=0.3 m pipe with sand with a d_{50} of 0.77 mm, concentrations up to 16%, inclination angles up to 44° and line speeds up to 7 m/s.

The physics of slurry transport can be divided into 5 main flow regimes. Each flow regime has its dominating physics. The stationary bed regime is based on bed friction, the sliding bed flow regime on sliding friction, the heterogeneous flow regime on collisions and collision intensity, the homogeneous flow regime on wall friction and the sliding flow regime on sliding friction. So, each flow regime requires its own approach how to deal with inclined pipes. Models in literature most often multiply the so-called solids effect with the cosine of the inclination angle, without considering different flow regimes, which is considered here as incorrect. Because different flow regimes respond differently, also the transitions between the flow regimes will depend on the inclination angle. It should be noted however that the potential energy term always dominates the hydraulic gradients measured.

Keywords: Slurry transport, inclined pipes, flow regimes.

INTRODUCTION

The research question here is, what is the influence of the inclination angle on the hydraulic gradient, on the Limit of Stationary Deposit Velocity (LSDV) and on the Limit Deposit Velocity (LDV). The effect of inclined pipes is expressed based on the length of the pipe, not the horizontal distance. The hydraulic gradient is a dimensionless number, used by most researchers to express pressure losses in pipes. By

---

[1] Associate Professor, Delft University of Technology, Mekelweg 2, 2628 CD, Delft, The Netherlands, T: ++31-15-2788359, Email: s.a.miedema@tudelft.nl.

[2] Senior engineer, CCCC National Engineering Research Center of Dredging Technology and Equipment, China. Email: wangfeixin@cccc-drc.com.

[3] Senior engineer, CCCC National Engineering Research Center of Dredging Technology and Equipment, China. Email: hongguojun@cccc-drc.com.

[4] PhD Candidate, Offshore and Dredging Engineering, Delft University of Technology. Email: x.chen-1@tudelft.nl.

dividing the pressure losses by the carrier liquid density and the length of the pipeline, a very convenient dimensionless number is found.

$$i = \frac{\Delta p}{\rho_l \cdot g \cdot \Delta L} \quad \text{with} \quad i_l = \frac{\Delta p_l}{\rho_l \cdot g \cdot \Delta L} = \frac{\lambda_l \cdot \frac{\Delta L}{D_p} \cdot \frac{1}{2} \cdot \rho_l \cdot v_{ls}^2}{\rho_l \cdot g \cdot \Delta L} = \frac{\lambda_l \cdot v_{ls}^2}{2 \cdot g \cdot D_p} \tag{1}$$

Another very convenient dimensionless number is the relative solids effect, given by:

$$E_{rhg} = \frac{i_m - i_l}{R_{sd} \cdot C_v} = \frac{\Delta p_m - \Delta p_l}{\rho_l \cdot g \cdot \Delta L \cdot R_{sd} \cdot C_v} \quad \text{with} \quad R_{sd} = \frac{\rho_m - \rho_l}{\rho_l} = \frac{\rho_m}{\rho_l} - 1 \tag{2}$$

Before focusing on the DHLLDV Framework, first several models/equations from literature are shown.

The Heterogeneous Flow Regime, Durand & Condolios and Gibert.

The basic equation for the solids effect of Durand & Condolios (1952) and Gibert (1960) for inclined pipes, is adding the cosine of the inclination angle according to:

$$i_{m,\theta} = i_l + \sin(\theta) \cdot (1 + R_{sd} \cdot C_{vt}) + i_l \cdot 81 \cdot \left(\frac{v_{ls}^2 \cdot \sqrt{C_x}}{g \cdot D_p \cdot R_{sd}} \right)^{-3/2} \cdot C_{vt} \cdot \cos(\theta)^{3/2} \tag{3}$$

The first term in this equation is the Darcy Weisbach hydraulic gradient for the carrier liquid. The second term is the potential energy term for both the carrier liquid and the solids. The third term is the solids effect term. So, the solids effect is multiplied with the cosine of the inclination angle to the power of 3/2. This means the solids effect is decreasing with an increasing inclination angle, whether the inclination is upwards or downwards. It should be mentioned that the hydraulic gradient is based on the length of the pipe and not on the horizontal component of the length.

The Heterogeneous Flow Regime, Worster & Denny.

Worster & Denny (1955) have a slightly different approach. They state that the hydraulic gradient in an inclined pipe equals the sum of the hydraulic gradients of the horizontal component and the vertical component. This gives the following equation:

$$i_{m,\theta} = i_l + \sin(\theta) \cdot (1 + R_{sd} \cdot C_{vt}) + i_l \cdot 81 \cdot \left(\frac{v_{ls}^2 \cdot \sqrt{C_x}}{g \cdot D_p \cdot R_{sd}} \right)^{-3/2} \cdot C_{vt} \cdot \cos(\theta) \tag{4}$$

The difference with Durand & Condolios (1952) and Gibert (1960) is the power of the cosine. In both cases, the equations match the hydraulic gradient of a horizontal pipe if the inclination angle equals zero and a vertical pipe if the inclination angle equals 90 degrees, whether the inclination is upwards (positive inclination angle) or downwards (negative inclination angle). However, in both cases, the Equivalent Liquid Model (ELM) component for a vertical pipe is missing.

The Heterogeneous Flow Regime, Wilson et al.

For inclined pipes, Wilson et al. (2006) modified the equation for horizontal pipes, matching the reasoning of Worster & Denny (1955), but with the use of the power M according to:

$$i_{m,\theta} = i_l + \sin(\theta) \cdot (1 + R_{sd} \cdot C_{vt}) + \frac{\mu_{sf}}{2} \cdot \left(\frac{v_{50}}{v_{ls}}\right)^M \cdot R_{sd} \cdot C_{vt} \cdot \cos(\theta)^M \quad (5)$$

The power M has a value of 1.7 for uniform or narrow graded sands and decreases to 0.25 for very broad graded sands. For narrow graded sands the influence of the inclination angle is similar to the Durand & Condolios (1952) and Gibert (1960) approach with a power of 1.5 versus 1.7 for Wilson et al. (2006). For medium graded sands with a power around 1, the influence is like the Worster & Denny (1955) approach.

The Sliding Bed Regime, Doron et al.

Doron et al. (1997) investigated the influence of inclined pipes, based on their 2LM and 3LM models (LM=Layer Model). Basically, they multiplied the sliding friction with the cosine of the inclination angle, and they added the potential energy term, which is proportional with the sine of the inclination angle. They carried out experiments with inclination angles from -7 to +7 degrees. The resulting data however is dominated by the potential energy term, because of the small inclination angles.

DISCUSSION OF LITERATURE

After adding the potential energy terms to the hydraulic gradient in a correct way, the pipe inclination effect can be considered, by multiplying the solids effect term with the cosine of the inclination angle to a power ranging from 1.0 to 1.7. Different researchers give different powers, most probably because the models are either empirical or have different physical backgrounds. This implies that the solids effect reduces to zero for a vertical pipe, which is doubtful, especially for very small particles giving homogeneous flow (ELM). One would expect an equation of the following form:

$$i_{m,\theta} = i_l \cdot \left(1 + \alpha \cdot R_{sd} \cdot C_{vs} \cdot \sin(\theta)^{\beta_1}\right) + \sin(\theta) \cdot (1 + R_{sd} \cdot C_{vs}) + E_{rhg} \cdot R_{sd} \cdot C_{vs} \cdot \cos(\theta)^{\beta_2} \quad (6)$$

The first term on the right-hand side is the Darcy Weisbach friction, including the mobilized ELM (the homogeneous solids effect) corrected for the inclination angle. The second term is the potential energy term. The third term is the solids effect ($E_{rhg)}$) corrected for the inclination angle. So, where the solids effect decreases with the inclination angle, the homogeneous solids effect increases. In this form a vertical pipe shows mobilized/reduced ELM behavior, which is observed by Newitt et al. (1961). Other flow regimes were not considered. Although this equation is a big improvement compared to the equations from literature, it does not yet distinguish explicitly between the flow regimes.

DHLLDV FRAMEWORK MODELING

The DHLLDV Framework combines the 5 flow regimes into one hydraulic gradient or relative solids effect curve. Figure 1~~Figure 1~~ shows the definitions used in a cross section of the pipe used for the stationary and sliding bed flow regimes. A short summary of each flow regime is given, since Miedema (2017C) already explained the detailed derivation for each flow regime.

Pure Carrier Liquid in an Inclined Pipe

The hydraulic gradient for pure carrier liquid in an inclined pipe can now be determined with:

$$i_{l,\theta} = i_l + \sin(\theta) \quad (7)$$

So apparently, the hydraulic gradient increases with the sine of the inclination angle. Which also means that a downwards slope with a negative inclination angle gives a negative sine and thus a reduction of the hydraulic gradient. In this case the hydraulic gradient may even become negative.

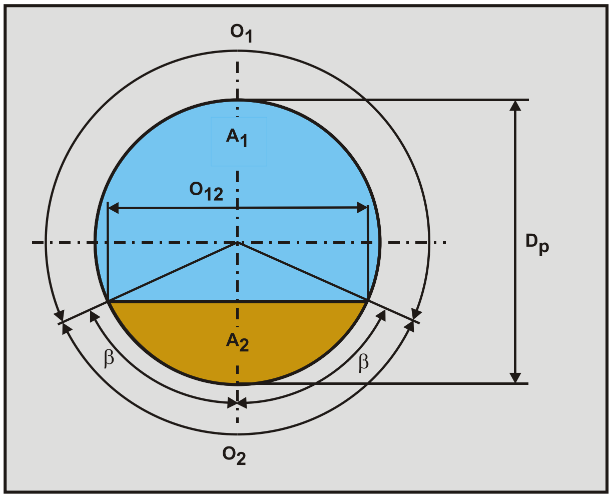

Figure 1: Definitions.

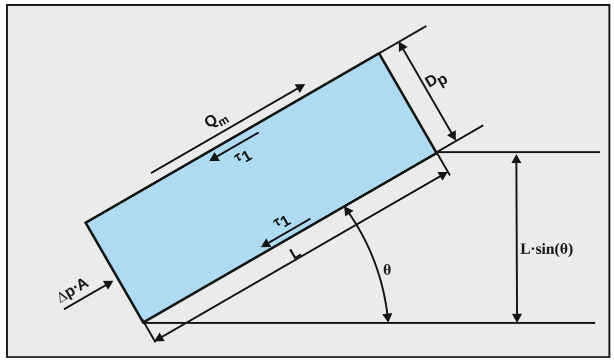

Figure 2: Pure carrier liquid in an inclined pipe.

Stationary Bed Regime in an Inclined Pipe

Since the bed is not moving, the friction between the bed and the pipe wall compensates for the weight component of the bed. The hydraulic gradient can now be determined with:

$$i_{m,\theta} = \frac{\tau_1 \cdot O_1 \cdot L + \tau_{12} \cdot O_{12} \cdot L}{\rho_l \cdot A_1 \cdot L \cdot g} + \sin(\theta) = i_m + \sin(\theta) \tag{8}$$

Which is the hydraulic gradient of a stationary bed in a horizontal pipe plus the sine of the inclination angle. The weight of the solids does not give a contribution to the hydraulic gradient, since the solids are not moving. See Figure 3: The stationary bed regime in an inclined pipe.~~Figure 3: The stationary bed regime in an inclined pipe.~~

Sliding Bed Regime in an Inclined Pipe

The hydraulic gradient for the sliding bed regime is:

$$i_{m,\theta} = i_l + \sin(\theta) \cdot (1 + R_{sd} \cdot C_{vs}) + R_{sd} \cdot C_{vs} \cdot \mu_{sf} \cdot \cos(\theta) \tag{9}$$

The relative excess hydraulic gradient or relative solids effect $\mathbf{E_{rhg,\theta}}$ is now:

$$E_{rhg,\theta} = \frac{i_{m,\theta} - i_{l,\theta}}{R_{sd} \cdot C_{vs}} = \mu_{sf} \cdot \cos(\theta) + \sin(\theta) \tag{10}$$

See: Figure 4: The submerged weight components and the sliding bed friction force.~~Figure 4: The submerged weight components and the sliding bed friction force.~~and Figure 5: A sliding bed in an inclined pipe.~~Figure 5: A sliding bed in an inclined pipe.~~

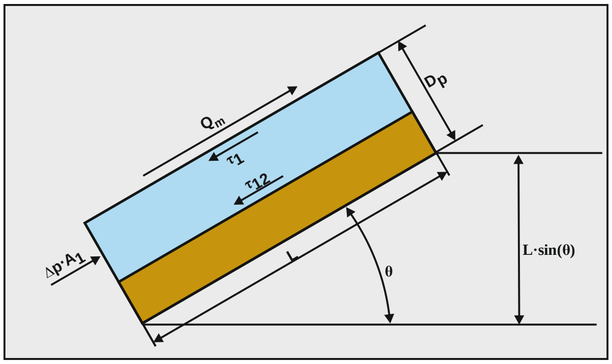

Figure 3: The stationary bed regime in an inclined pipe.

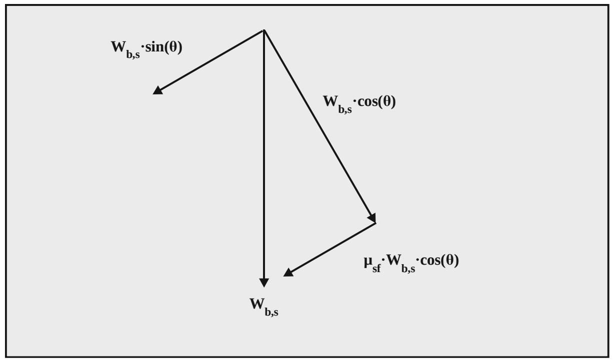

Figure 4: The submerged weight components and the sliding bed friction force.

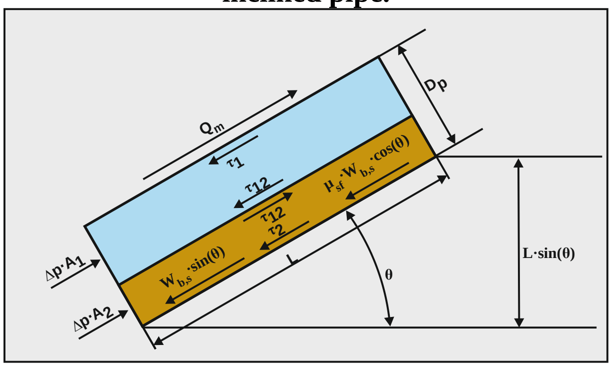

Figure 5: A sliding bed in an inclined pipe.

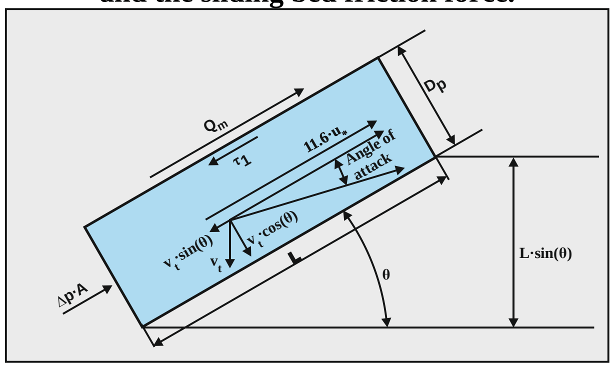

Figure 6: Heterogeneous flow in an inclined pipe, the angle of attack.

Heterogeneous Regime in an Inclined Pipe

In an inclined pipe the effective terminal settling velocity perpendicular to the pipe wall gives a potential energy term of:

$$S_{hr,\theta} = S_{hr} \cdot \cos(\theta) = \frac{v_t \cdot \left(1 - \frac{C_{vs}}{\kappa_C}\right)^{\beta}}{v_{ls}} \cdot \cos(\theta) \tag{11}$$

For the kinetic energy losses, the angle of attack has to be adjusted in an inclined pipe. The angle of attack is defined as the ratio between the terminal settling velocity and the velocity at the thickness of the viscous sub layer, giving (see Figure 6~~Figure 6~~):

$$S_{rs,\theta} = c \cdot \left(\frac{\delta_v}{d}\right)^{2/3} \cdot \left(\frac{v_t \cdot \cos(\theta)}{11.6 \cdot u_* - v_t \cdot \sin(\theta)}\right)^{4/3} \cdot \left(\frac{v_t}{\sqrt{g \cdot d}}\right)^{2} \tag{12}$$

So, for very small particles with $\mathbf{v_t << 11.6 \cdot u_*}$, the kinetic energy losses are proportional to the cosine of the inclination angle to a power of 4/3. For larger particles, the term in the denominator becomes significant resulting in different behavior of a positive versus a negative inclination angle. Apart from this, also the lifting of the mixture has to be added, giving:

$$
\begin{aligned}
& i_{m,\theta} = i_l + \sin(\theta) \cdot (1 + R_{sd} \cdot C_{vs}) + (S_{hr,\theta} + S_{rs,\theta}) \cdot R_{sd} \cdot C_{vs} \\
& E_{rhg,\theta} = S_{hr,\theta} + S_{rs,\theta} + \sin(\theta)
\end{aligned}
\tag{13}
$$

Literature shows a power of the cosine between 1 and 1.7. Here a more complicated formulation is found. Considering that the potential energy losses are much smaller than the kinetic energy losses, a power of about 4/3 is found for small particles, while larger particles will show a smaller power depending on the terminal settling velocity (see equation (12)~~(12)~~). The higher the terminal settling velocity, the smaller the power. Theoretically this power may even become zero when nominator and denominator decrease in the same way with increasing inclination angle.

Homogeneous Regime in an Inclined Pipe

For an inclined pipe, only the lifting of the mixture must be added, giving:

$$
\begin{aligned}
& i_{m,\theta} = i_l \cdot (1 + \alpha_E \cdot R_{sd} \cdot C_{vs}) + \sin(\theta) \cdot (1 + R_{sd} \cdot C_{vs}) \\
& E_{rhg,\theta} = \alpha_E \cdot i_l + \sin(\theta)
\end{aligned}
\tag{14}
$$

Sliding Flow Regime or Fully Stratified Flow in an Inclined Pipe

The sliding flow regime behaves the same as the sliding bed regime, since both regimes are dominated by sliding friction, so:

$$
i_{m,\theta} = i_l + \sin(\theta) \cdot (1 + R_{sd} \cdot C_{vs}) + R_{sd} \cdot C_{vs} \cdot \mu_{sf} \cdot \cos(\theta) \tag{15}
$$

The relative excess hydraulic gradient or relative solids effect $\mathbf{E_{rhg,\theta}}$ is now:

$$
E_{rhg,\theta} = \frac{i_{m,\theta} - i_{l,\theta}}{R_{sd} \cdot C_{vs}} = \mu_{sf} \cdot \cos(\theta) + \sin(\theta) \tag{16}
$$

The Limit Deposit Velocity

The Limit of Stationary Deposit Velocity is affected by the pipe inclination. In an ascending pipe, the cross-sectional averaged line speed has to be higher compared to a horizontal pipe in order to make a bed start sliding. In a descending pipe this line speed is lower. It is even possible that in a descending pipe the bed will always slide because of gravity. The Limit of Stationary Deposit Velocity is at the transition of the stationary bed regime and the sliding bed regime. The Limit Deposit Velocity, defined as the line speed above which there is no stationary or sliding bed, is determined by either the potential energy losses or a limiting sliding bed. In both cases this is affected by the cosine of the inclination angle, the component of gravity perpendicular to the pipe wall. Since in both cases the Limit Deposit Velocity depends on the cube root of this cosine, the Limit Deposit Velocity will decrease according to Miedema (June 2016):

$$
v_{ls,ldv,\theta} = v_{ls,ldv} \cdot \cos(\theta)^{1/3} \tag{17}
$$

Because of the cube root of this cosine, this means that for angles up to 45º the reduction is less than 10%.

DISCUSSION OF MODELING

For the stationary bed regime, only the potential energy term of the pure liquid must be added to the hydraulic gradient of the mixture (basically the pure liquid hydraulic gradient in the restricted area above the bed). For all other flow regimes, the potential energy term of the mixture must be added, together with a correction of the so-called solids effect. The result of this is a higher line speed for the intersection point of the stationary bed curve and the sliding bed curve. So, in general an increase of the Limit of Stationary Deposit Velocity (LSDV) with increasing inclination angle. This may however also result in omission of the occurrence of a sliding bed for an inclined pipe, where a sliding bed would occur in a horizontal pipe. This makes sense, since a higher line speed is required to make a bed start sliding, there is the possibility that the bed is already fully suspended before it could start sliding. With negative inclination angles, a stationary bed may never occur if the arctan of the sliding friction coefficient of the sand with the pipe wall is smaller than the inclination angle. Usually this sliding friction angle or angle of external friction will be about 20°. So, if the descending inclination angle is smaller than -20°, the LSDV does not exist and even at zero-line speed the bed is already sliding. This is also the reason why the Wilson et al. (2006) graph for the correction for inclined pipes starts at -20°.

In the sliding bed/sliding flow regime and the heterogeneous regime, the hydraulic gradient is lower for an inclined pipe compared with a horizontal pipe, if the potential energy term of the mixture (static head) is not considered, especially for small particles in the heterogeneous regime. For the heterogeneous regime, there is a difference between ascending and descending pipes, due to the term with the angle of attack in the kinetic energy losses. The decrease in an ascending pipe is smaller than in a descending pipe and could even give a small increase in an ascending pipe at low line speeds. The transition line speed of the heterogeneous flow regime to the homogeneous flow regime will also decrease with increasing inclination angle.

In case of a sliding bed one may expect more stratification in an ascending pipe compared to a descending pipe, due to the higher line speed in an ascending pipe to make the bed start sliding. In other words, a higher shear stress on the bed is required in an ascending pipe, resulting in a thicker sheet flow layer at the top of the bed.

The hydraulic gradients of the inclined pipes are determined per meter of inclined pipe and not per meter of horizontal pipe. In order to find the correct hydraulic gradient curves for an inclined pipe, one first has to determine the hydraulic gradient curves for each flow regime individually. The resulting curve can be found by comparing flow regime curves with the line speed as a variable.

1. If the sliding bed hydraulic gradient (SB) is smaller than the stationary (fixed) bed hydraulic gradient (FB), the sliding bed hydraulic gradient (SB) is chosen, otherwise the stationary (fixed) bed hydraulic gradient (FB). The resulting curve is named the **FB-SB** curve, or in a descending pipe with an angle smaller than about -20°, the **SB** curve
2. In the case of sliding flow (SF, large particles), $\mathbf{d>0.015\cdot D_p}$ according to Wilson et al. (2006), this is also the final curve (see Miedema (2018A) and (2018B) for a more detailed criterion). This curve is named the **FB-SB-SF** curve, or in a descending pipe with an angle smaller than about -20°, the **SB-SF** curve. If there is no sliding flow (small and medium sized particles) steps 3 and 4 must be taken.
3. If the heterogeneous flow regime hydraulic gradient (He) is smaller than the FB-SB hydraulic gradient, the heterogeneous hydraulic gradient (He) is chosen, otherwise the FB-SB hydraulic gradient. The resulting curve is named the **FB-SB-He** curve, or in a descending pipe with an angle smaller than -20°, the **SB-He** curve. Depending on the parameters (particle and pipe diameter), it is possible that this curve does not contain a sliding bed regime. In that case the resulting curve is the **FB-He** curve. The particles will be so small that sliding flow will not occur in this case.
4. If there is no sliding flow and the homogeneous flow regime hydraulic gradient (Ho) is larger than the FB-SB-He hydraulic gradient, the homogeneous hydraulic gradient (Ho) is chosen, otherwise the FB-

SB-He or FB-He hydraulic gradient. The resulting curve is named the **FB-SB-He-Ho** curve, or in a descending pipe with an angle smaller than -20°, the **SB-He-Ho** curve.

It may be clear that the resulting hydraulic gradient curves do not respond in a single way to the inclinations angle, since each flow regime has its own characteristic behavior. This implies that the models from literature are not useable, since the Durand & Condolios (1952) , Worster & Denny (1955) and Wilson et al. (2006) models are created only for the heterogeneous flow regime and constant transport concentration, while the Doron & Barnea (1997) model was created for a sliding bed and constant spatial concentration. The reality seems to be more complicated.

VALIDATION

De Vreede (2018), carried out experiments at the National Engineering Research Center for Dredging (NERCD) in Shanghai. The experiments were carried out with a flow loop with a pipe diameter of 300 mm. It contains a measurement section of over 110 meters, part of which is inclinable. Pipe inclination angles of 17.9, 28.9 and 44 degrees were tested with slurry concentrations up to 15 % at flow velocities between 2 and 7 m/s. The sand used in the experiments had a d_{50} of 0.77 mm on average. The flow velocities (line speeds), delivered concentrations, total pressures, differential pressures and pump data were recorded. Conducting these experiments on this scale under controlled laboratory conditions is a unique research. Figure 7 gives a schematic display of the test setup

In Figure 7 the slurry would "start" at the slurry tanks (1) (not displayed). Upstream from the slurry tanks, the water reservoir is located. The slurry tanks and water reservoir are connected via a set of pipes and valves. The pump is located at 2, downstream from the reservoirs in the figure. Directly after the pump a section that serves as a U-loop (3) is found. The U-loop is outfitted with 2 differential pressure meters (one on each leg) and an ultrasonic density meter. After the U-loop, the pipe is led through a water basin (4) that can serve as cooling section. From the cooling system, the pipe is led upwards where the electromagnetic flow meter (5) is attached to the vertical ascending leg of the vehicle crossing. Directly downstream from the vehicle crossing, the inclinable segment (6) starts with the ascending section, then a 180 degree turn and the descending section. Several differential pressure meters and total pressure sensors are attached to it. The horizontal section (7) begins right after the inclinable segment downstream from the descending section. This horizontal section includes differential pressure meters and total pressure sensors. The horizontal pipe has a Perspex observation section built in to monitor sliding or stationary beds. After the horizontal measurement section, the second 180 degree turn (8) is located which leads the flow led back to the slurry tanks. The ascending and descending legs of the inclinable section have a combined maximum length of approximately 50 meters depending on the inclination angle. At inclination angles over 18 degrees, the inclinable section is shortened to fit under the roof of the laboratory. The horizontal measurement section excluding the inclinable section is a little under 60 meters long. Except for the connections at the slurry reservoir, the pipe diameter of the whole setup is 300 mm. Figure 8 shows the inclinable sections with inclination angles of 20, 30 and 45 degrees, both ascending and descending. Because the top of the inclinable section did not completely fit in the building, the angles used were slightly smaller, 17.9, 28.9 and 44 degrees. The lengths of the inclinable sections are 11.5 m, 17.5 m and 26.5 m. A detailed description of the experimental setup including the transducers and measurement methods used can be found in de Vreede (2018).

The experiments were carried out with intended constant delivered concentrations of 0%, 2.5%, 5%, 7.5%, 10% and 12.5%. In reality, it was difficult to obtain constant delivered concentrations during the experiments. First of all, the delivered concentrations were measured in the U-loop and not in the inclinable section, so there may have been a difference, because in the U-loop there will never be any bed forming while in the inclinable section there might. Especially at low line speeds. Based on the way the experiments were carried out, an almost constant amount of solids in the whole system, the assumption of an almost constant spatial volumetric concentration is more realistic. This spatial concentration is also required in the DHLLDV model described here. Still there are differences in the concentration between the experiments at different inclination angles. Since the inclinable section contains both the ascending and the descending pipe and the hydraulic gradients were measured simultaneously, there may have been a difference in the spatial concentrations between the ascending and descending pipes. It is likely that the ascending pipe had a slightly higher spatial concentration compared with the descending pipe, especially at low line speeds. The experimental data has been corrected for these effects, based on the potential energy component of the hydraulic gradient, since this component does not depend on the modelling of the solids effect. The resulting hydraulic gradients are shown in Figure 10, Figure 11, Figure 12, Figure 13, Figure 14 and Figure 15. The actual spatial volumetric concentrations used in the graphs are 0%, 2%, 5%, 7.5%, 10% and 13.5%.

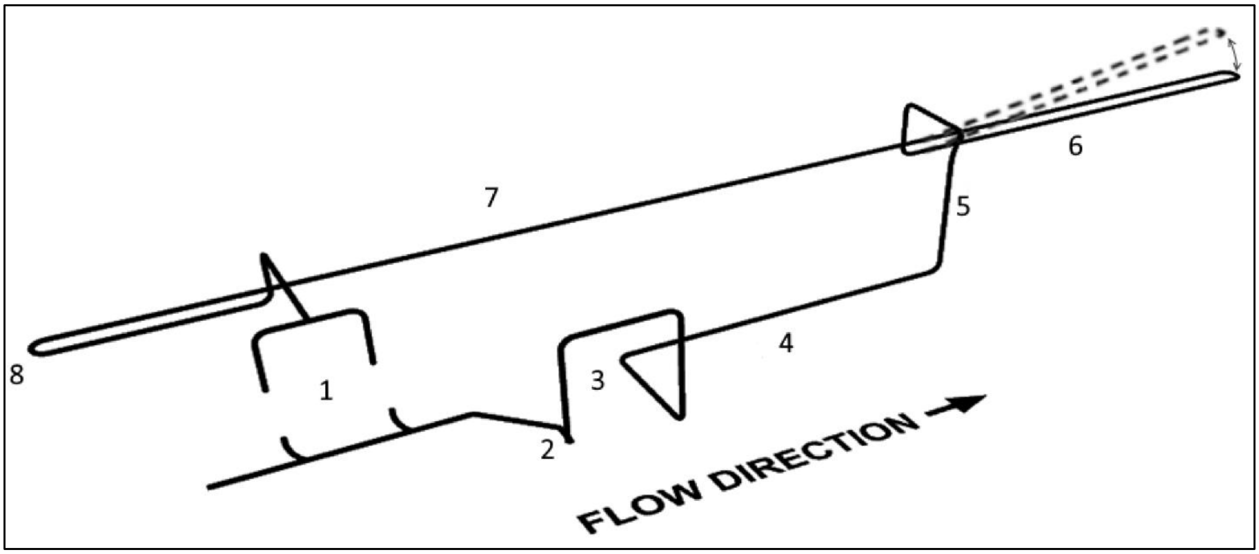

Figure 7: Schematic display of the test setup (source: de Vreede (2018)).

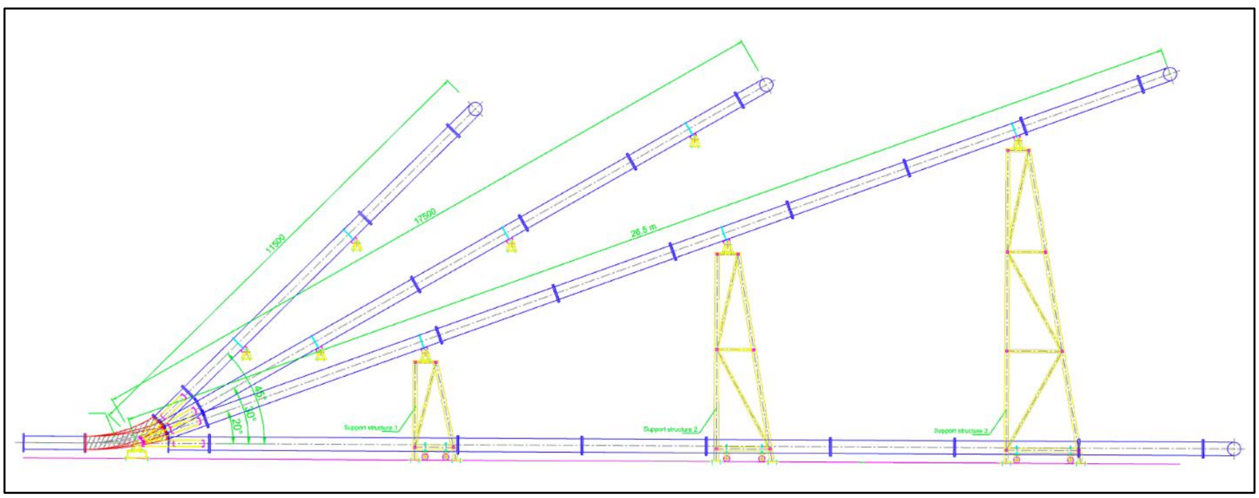

Figure 8: The inclinable section with inclination angles of 20, 30 and 45 degrees (source: de Vreede (2018)).

Figure 10 shows the hydraulic gradient curves and experimental data for pure liquid. The pipe wall roughness is calibrated based on these experiments, resulting in a good match. So, the theoretical assumption of the potential energy term for all inclined pipes seems to be valid. It should be mentioned here that it is always advised to check experimental data of something known, since there may be errors in the measurement.

Figure 9: The testing facility with the inclined loop.

The data points in the ascending pipe show a very good correlation with the theoretical curves, while the data points in the descending pipes show more scatter. Figure 11, Figure 12, Figure 13, Figure 14 and Figure 15 show the hydraulic gradient curves and experimental data for the mixtures. Based on the theory and the way the experiments were carried out, one may expect the following phenomena:

1. In the ascending pipes there will be a fixed bed regime at low line speeds, followed by the heterogeneous regime and the homogeneous regime (FB-He-Ho). The sliding bed regime will not occur due to the combination of particle and pipe diameters and the spatial concentrations. So, there is expected to be a direct transition from the fixed bed regime to the heterogeneous regime.
2. In the descending pipes there may be some fixed bed regime at very low line speeds at an inclination angle of -17.9°, followed by the sliding bed regime, the heterogeneous regime and the homogeneous regime. The inclination angle of -17.9° is already close to the expected friction angle of 20°. For the inclination angles of -28.9° and -44°, the sliding bed will already occur at zero line speed (compare with a brick on an inclined slope, the brick will start sliding if the inclination angle is larger than the friction angle). This sliding bed regime is followed by the heterogeneous regime and the homogeneous regime (SB-He-Ho).
3. Because of the layout of the circuit one may expect some accumulation of solids in the horizontal pipe sections at very low line speeds, resulting in a decrease of the spatial concentration in the inclinable sections. This will result in slightly lower hydraulic gradients at these low line speeds in the ascending pipe and slightly higher hydraulic gradients in the descending pipes, especially at the higher spatial concentrations.
4. Because of possible deceleration and accumulation in the ascending pipe and acceleration in the descending pipe, the spatial concentration in the ascending pipe may be slightly higher than in the descending pipe, resulting in some underestimation of the hydraulic gradient in the ascending pipe and in absolute value overestimation in the descending pipe, based on the overall average spatial concentration.

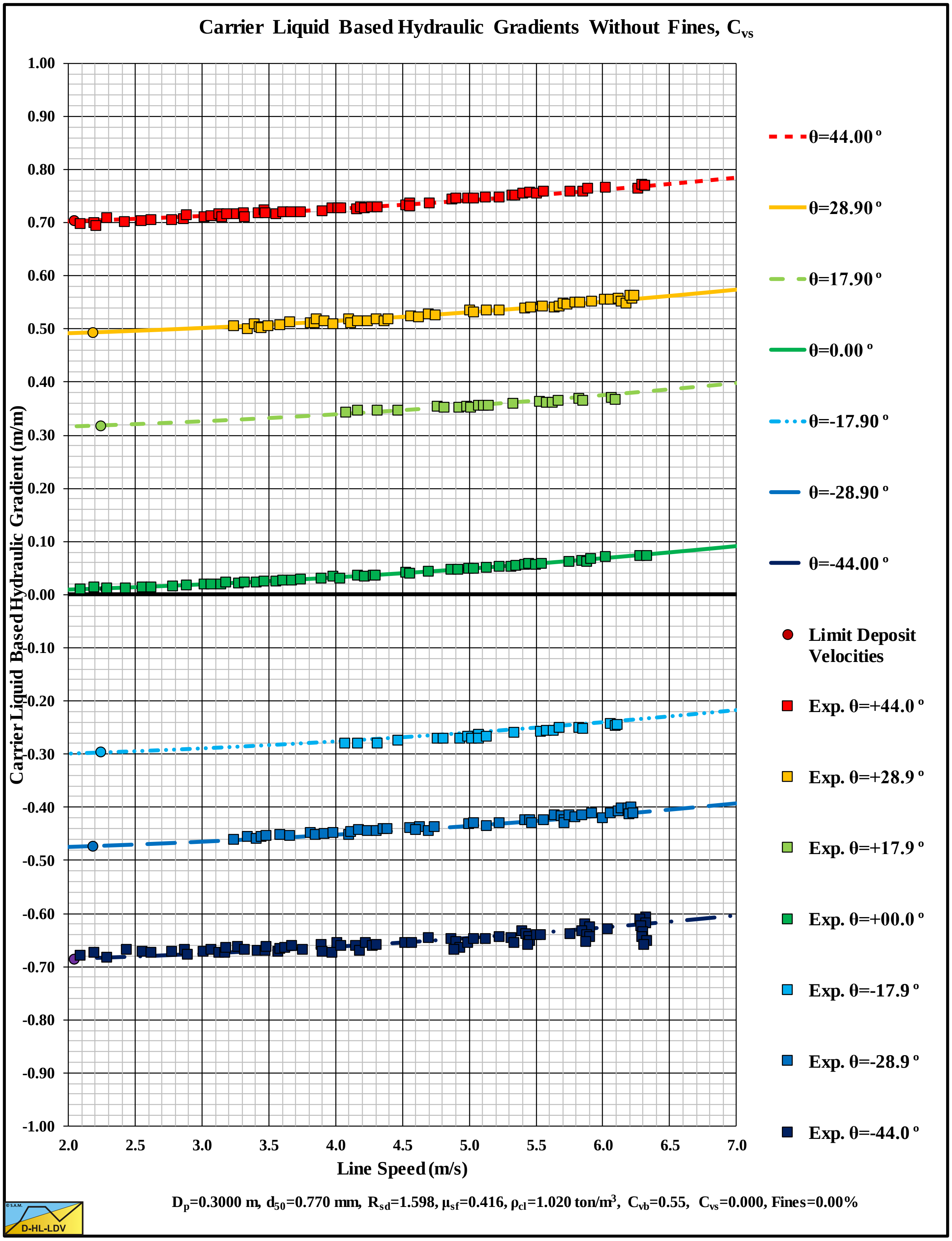

Figure 10: Inclined pipes C_{vs}=0.0%, experiments versus DHLLDV.

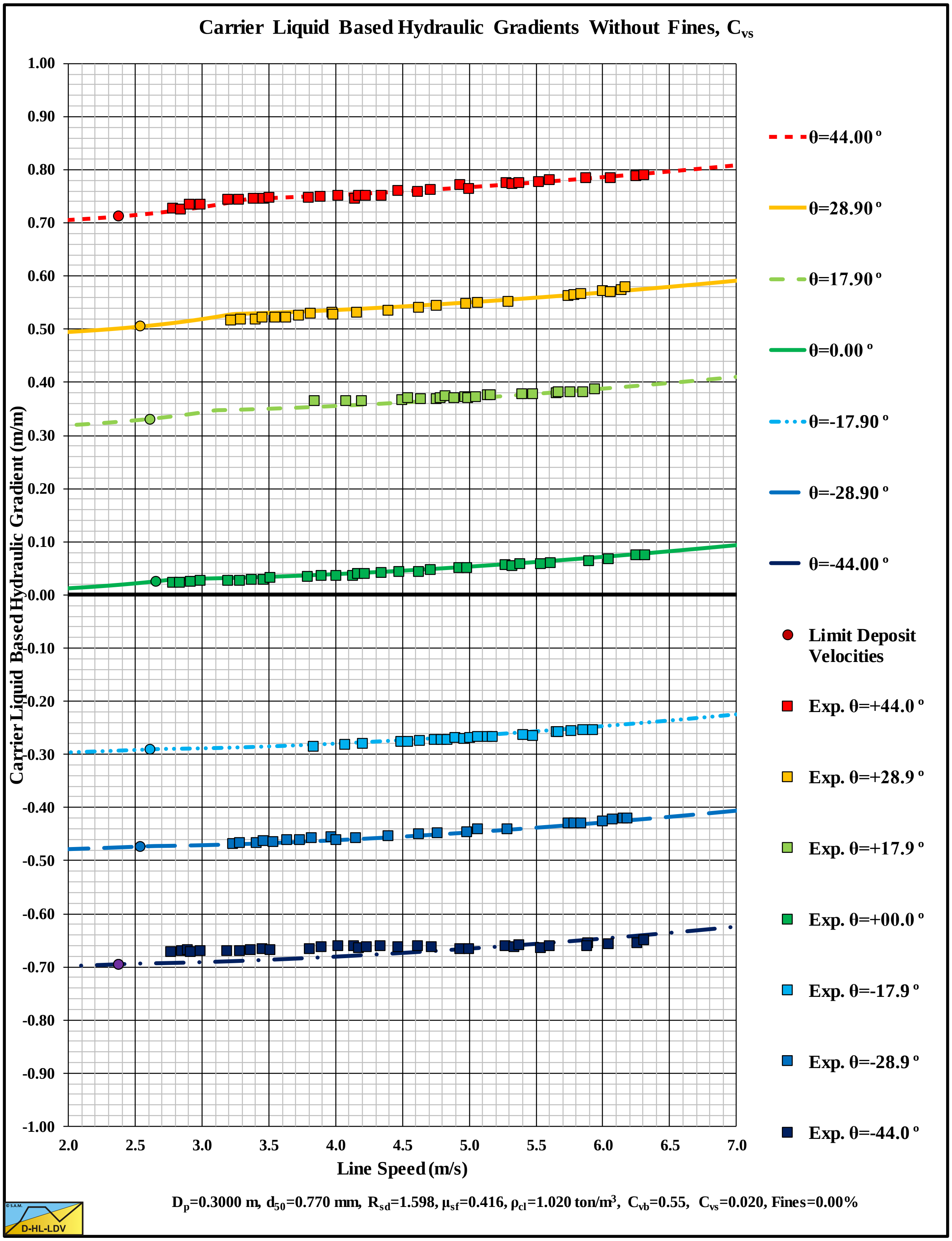

Figure 11: Inclined pipes C_{vs}=2.0%, experiments versus DHLLDV.

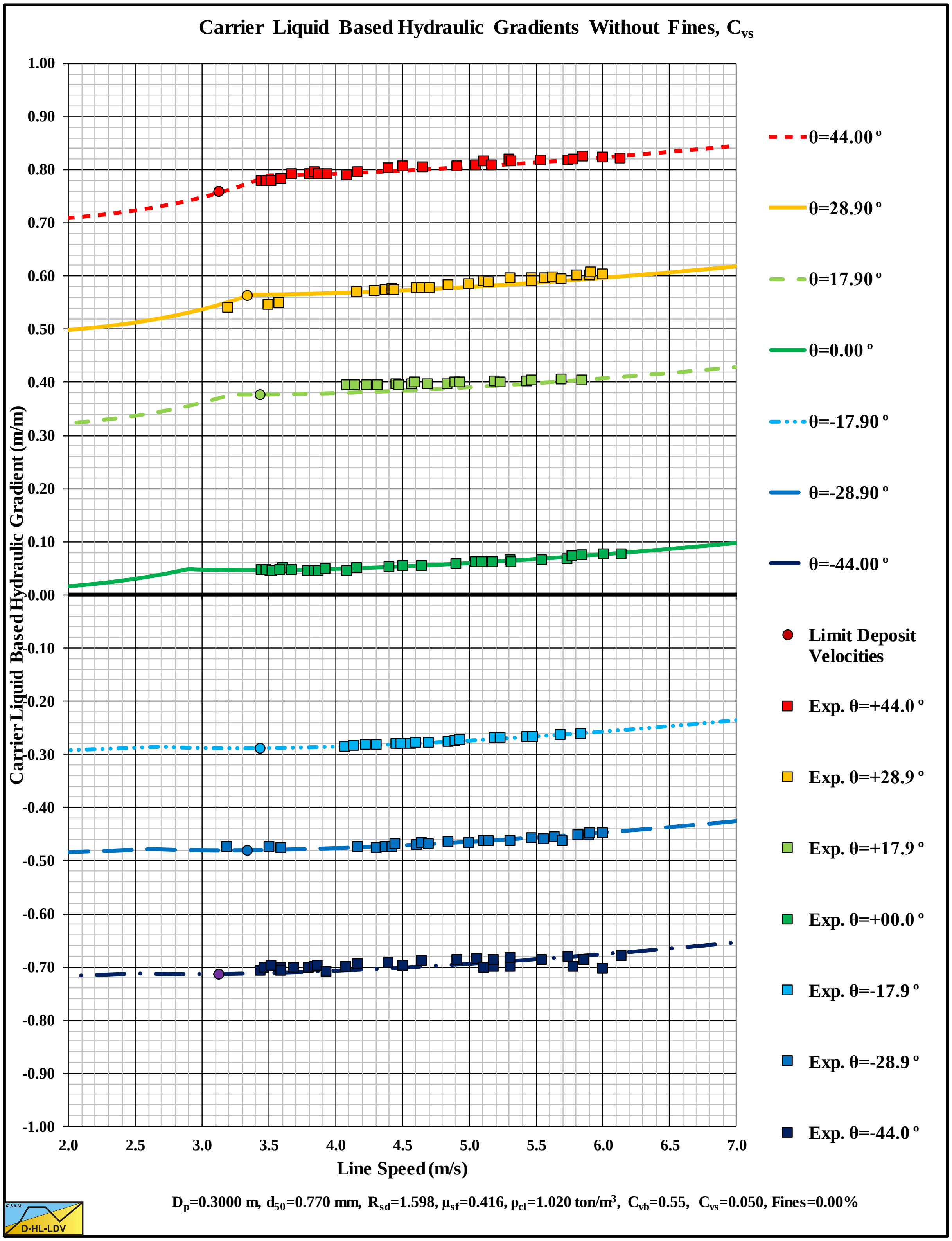

Figure 12: Inclined pipes C_{vs}=5.0%, experiments versus DHLLDV.

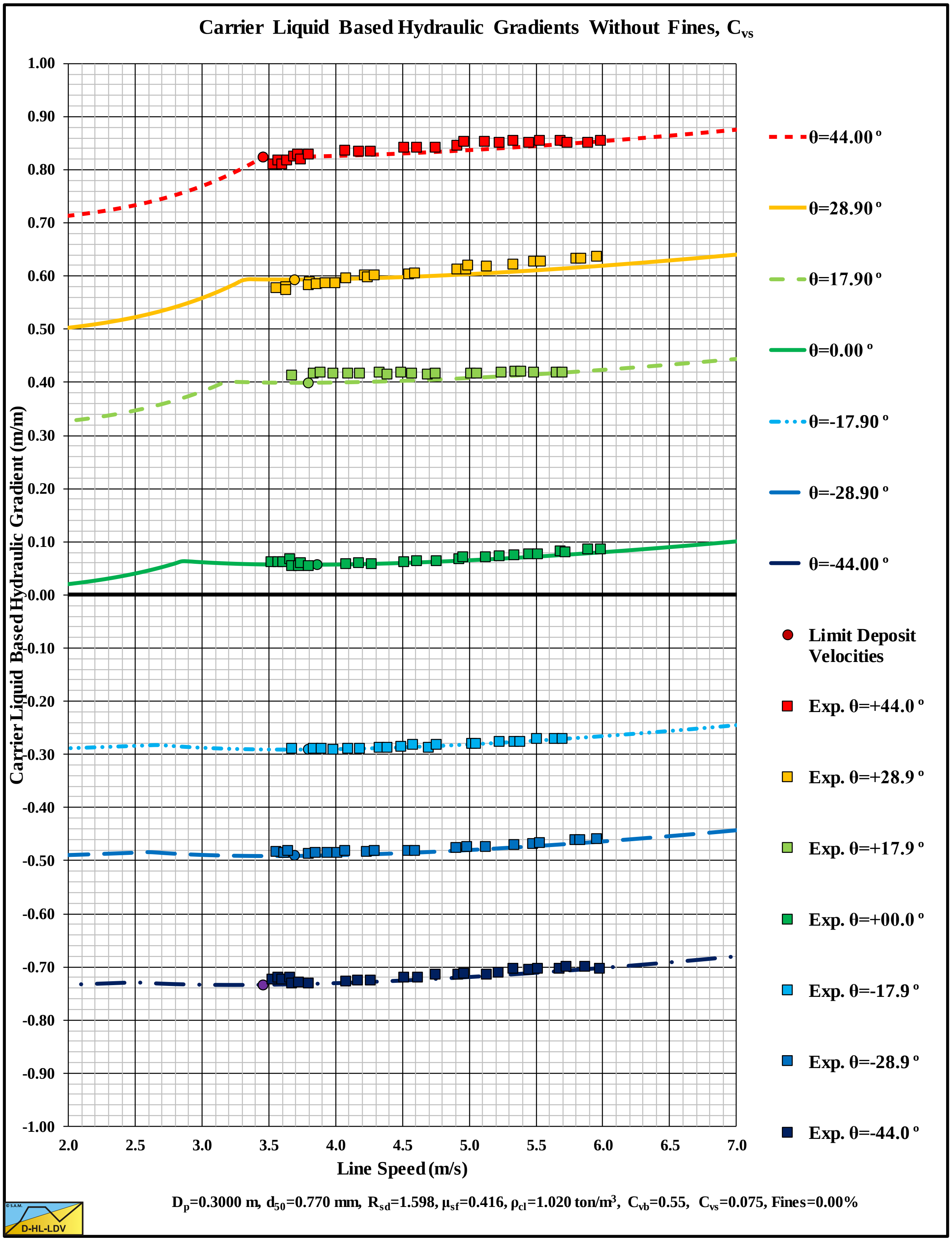

Figure 13: Inclined pipes C_{vs}=7.5%, experiments versus DHLLDV.

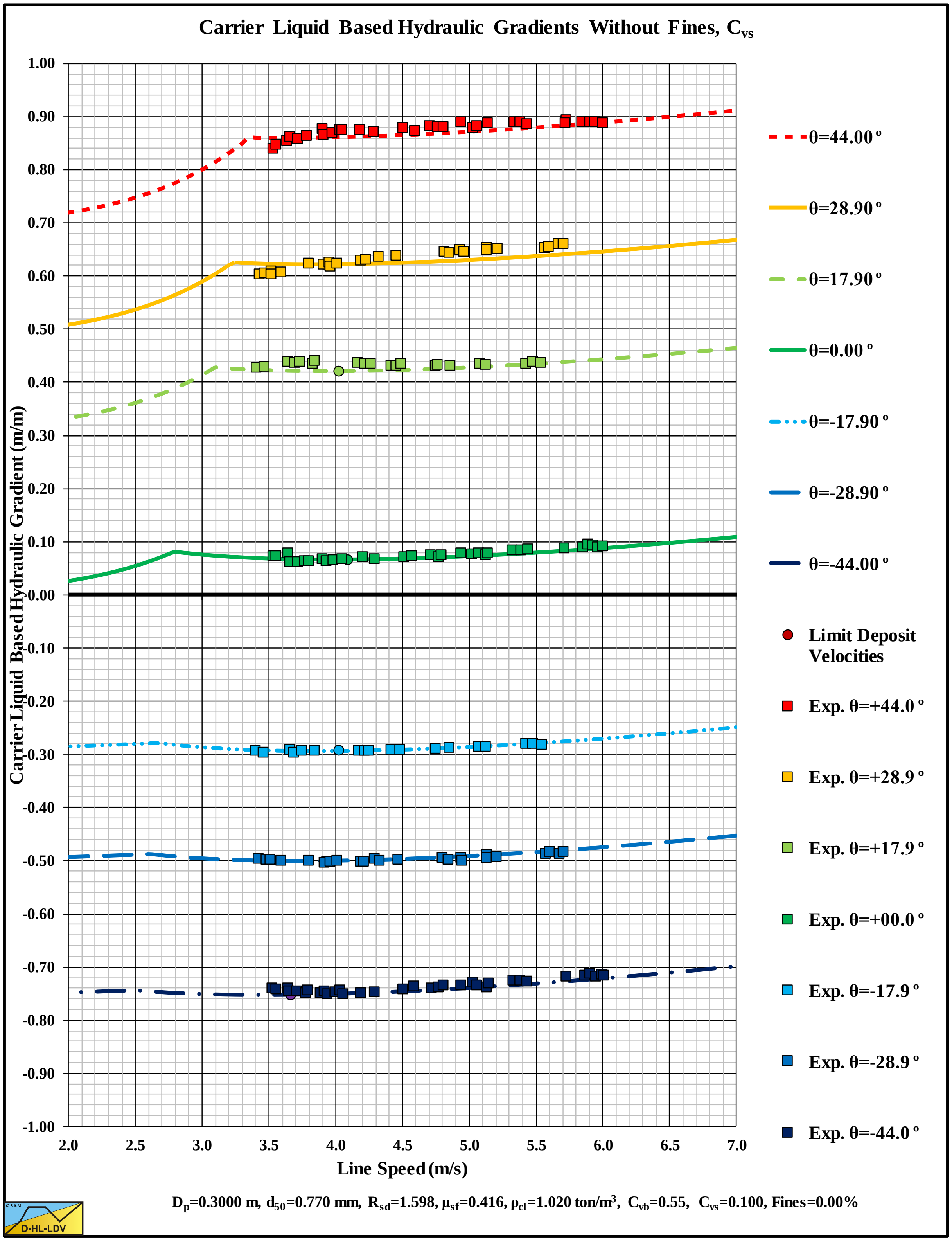

Figure 14: Inclined pipes C_{vs}=10.0%, experiments versus DHLLDV.

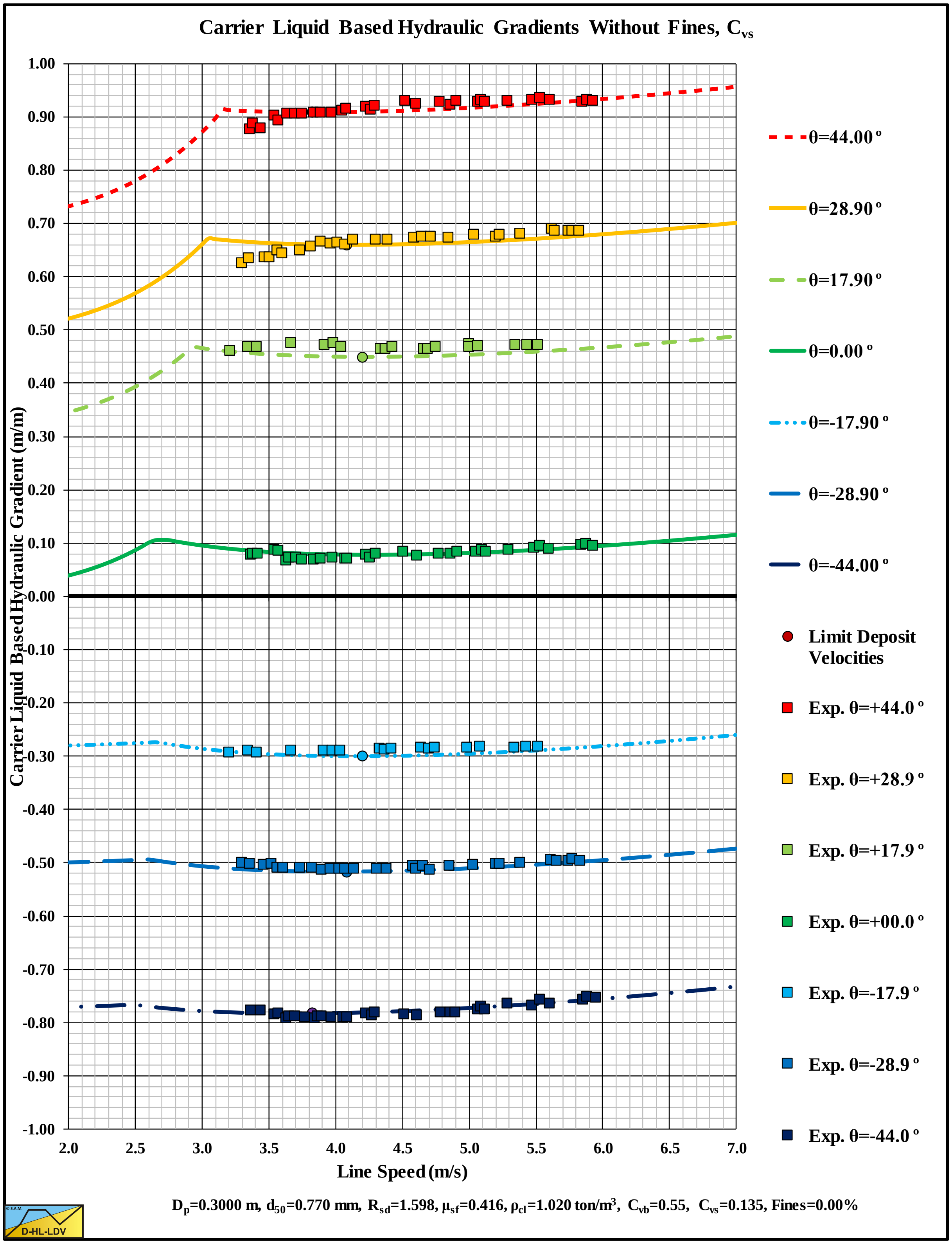

Figure 15: Inclined pipes C_{vs}=13.5%, experiments versus DHLLDV.

CONCLUSIONS & DISCUSSION

Models from literature multiply the so-called solids effect with the cosine of the inclination angle to a power between 0.25 and 1.7, based on the heterogeneous flow regime only or the sliding bed regime only. These models do not take the homogeneous (reduced) Equivalent Liquid Model (ELM) into consideration for very high inclination angles. The consequence is, that there is no solids effect in vertical pipes, which is doubtful.

The use of the cosine of the inclination angle on the solids effect for the sliding bed regime seems appropriate, a good first estimate. However, for the heterogeneous flow regime this is more complicated, resulting in a difference for an ascending compared to a descending pipe. In this case an ELM component containing the sine of the inclination angle should be added, however.

A proper model for inclined pipes should consider the different flow regimes individually and then combine the flow regime hydraulic gradients, based on which flow regime will occur at which line speed. The effect of the inclination angle may be different for the different flow regimes. Also, the transition line speeds between the different flow regimes depend on the inclination angle.

Since the occurrence of the different flow regimes depends strongly on the particle and pipe diameters and the line speed, this also has a dominant effect on the occurrence of the flow regimes in inclined pipes.

In an ascending pipe a bed will start sliding at a higher line speed and transit to heterogeneous flow at a lower line speed, with the possibility that there is no sliding bed at all, while there would be in a horizontal pipe. So, the line speed range of the sliding bed is reduced, possibly to zero. In a descending pipe the opposite will occur, with the possibility that there is a sliding bed from line speed zero up to the transition to heterogeneous transport.

The validation with the de Vreede (2018) experiments (CCCC National Engineering Research Center of Dredging Technology and Equipment, Shanghai, China) show a good correlation. However, it should be stated that the potential energy terms are dominating, and it is very difficult to identify the exact behavior of the solids effect. A good correlation means that the theoretical offset of the hydraulic gradient because of the potential energy matches the experiments, but also the shape of the theoretical hydraulic gradient curve matches the experiments, with sometimes some explainable deviation at low line speeds.

Now one could say, deduct the potential energy term and then compare the solids effect with the theory. This is possible; however, this would increase the scatter of the experimental data enormously in percentage. Also, because a small error in the spatial concentration would be magnified in the solids effect.

The approach chosen in the DHLLDV Framework as described here, determining hydraulic gradient curves for each flow regime and then combine/construct the resulting hydraulic gradient curve, seems to work very well.

NOMENCLATURE

A, A_p	Cross section pipe	**m^2**
A_1	Cross section restricted area above the bed	**m^2**
A_2	Cross section bed	**m^2**
c	Proportionality constant	**-**
C_{vb}	Bed volumetric concentration	**-**
C_{vs}	Spatial volumetric concentration	**-**
d	Particle diameter	**m**
E_{rhg}	Relative excess hydraulic gradient without pipe inclination	**-**
$E_{rhg,\theta}$	Relative excess hydraulic gradient with pipe inclination	**-**
g	Gravitational constant (9.81)	**m/s^2**
i_l	Hydraulic gradient liquid without pipe inclination	**-**
$i_{l,\theta}$	Hydraulic gradient liquid with pipe inclination	**-**
i_m	Hydraulic gradient mixture without pipe inclination	**-**
$i_{m,\theta}$	Hydraulic gradient mixture with pipe inclination	**-**
L	Length of pipe	**m**
O_1	Circumference restricted area above the bed in contact with pipe wall	**m**
O_2	Circumference of bed with pipe wall	**m**
O_{12}	Width of the top of the bed	**m**
p	Pressure in pipe	**kPa**
R_{sd}	Relative submerged density of solids	**-**
S_{hr}	Settling velocity Hindered Relative without pipe inclination	**-**
$S_{hr,\theta}$	Settling velocity Hindered Relative with pipe inclination	**-**
S_{rs}	Slip Ratio Squared without pipe inclination	**-**
$S_{rs,\theta}$	Slip Ratio Squared with pipe inclination	**-**
u_*	Friction velocity	**m/s**
v_{ls}	Line speed	**m/s**
v_t	Terminal settling velocity	**m/s**
v_{sl}	Slip velocity solids	**m/s**
$v_{ls,ldv}$	Limit Deposit Velocity without pipe inclination	**m/s**
$v_{ls,ldv,\theta}$	Limit Deposit Velocity with pipe inclination	**m/s**
W_b	Weight of the bed	**ton**
$W_{b,s}$	Submerged weight of the bed	**ton**
x	Distance in pipe length direction	**m**
α_E	Homogeneous lubrication factor	**-**
β	Richardson & Zaki hindered settling power	**-**
δ_v	Thickness viscous sub-layer	**m**
ρ_b	Density of the bed including pore water	**ton/m^3**
ρ_s	Density of the solids	**ton/m^3**
ρ_l	Density of the liquid	**ton/m^3**
ρ_m	Mixture density	**ton/m^3**
τ_1	Shear stress between liquid and pipe wall	**kPa**
τ_{12}	Shear stress on top of the bed	**kPa**
θ	Inclination angle (positive upwards, negative downwards)	**^{o}**
μ_{sf}	Sliding friction coefficient	**-**
κ_C	Concentration eccentricity factor	**-**

REFERENCES

Doron, P., Simkhis, M., & Barnea, D. (1997). Flow of solid liquid mixtures in inclined pipes. *International Journal of Multiphase Flow, Vol. 23, No. 2.*, 313-323.

Durand, R., & Condolios, E. (1952). Etude experimentale du refoulement des materieaux en conduites en particulier des produits de dragage et des schlamms. *Deuxiemes Journees de l'Hydraulique.*, 27-55.

Gibert, R. (1960). Transport hydraulique et refoulement des mixtures en conduites. *Annales des Ponts et Chausees.*, 130(3), 307-74, 130(4), 437-94.

Miedema, S. A. (2017C). Slurry transport in inclined pipes. *Dredging Summit & Expo* (p. 15). Vancouver, Canada: WEDA.

Miedema, S. A. (2018A). Slurry transport, fully stratified flow in the sliding flow regime. *Dredging Summit & Expo* (p. 15). Norfolk, Virginia, USA.: WEDA.

Miedema, S. A. (2018B). Slurry transport, the sliding flow regime or fully stratified flow. *Submitted to: Terra et Aqua*, 8.

Miedema, S. A. (June 2016). *Slurry Transport: Fundamentals, A Historical Overview & The Delft Head Loss & Limit Deposit Velocity Framework.* (1st Edition ed.). (R. C. Ramsdell, Ed.) Miami, Florida, USA: Delft University of Technology.

Newitt, D. M., Richardson, J. F., & Gliddon, B. J. (1961). Hydraulic conveying of solids in vertical pipes. *Transactions Institute of Chemical Engineers, Vol. 39.*, 93-100.

Ridder, J. K. (2018). *Horizontal slurry transport on a large laboratory scale.* Delft, the Netherlands: Delft University of Technology.

Ridder, J. K., Vreede, M. A., Wang, F., Talmon, A. M., & Chen, X. (2017). Preliminary results on the behavior of hydraulic transported solids through a horizontal pipeline in a large laboratory test setup. *5th International Dredging Technology Development Conference of China.* Beijing, China: CHIDA.

Vreede, M. d. (2018). *Hydraulic transport in inclined large diameter pipelines.* Delft, the Netherlands: Delft University of Technology.

Wilson, K. C., Addie, G. R., Sellgren, A., & Clift, R. (2006). *Slurry transport using centrifugal pumps.* New York: Springer Science+Business Media Inc.

Worster, R. C., & Denny, D. F. (1955). Hydraulic transport of solid materials in pipelines. *Institution of Mechanical Engineers (London)*, 563-586.

CITATION

Miedema, S.A., Wang, F., Hong, G. & Chen, X., "Dominating Factors in slurry transport in inclined pipes," *Proceedings of the Western Dredging Association Dredging Summit & Expo '20, Houston, TX, USA*, June 9-12, 2020.

DATA AVAILABILITY

All data and models generated or used during the study are included in the manuscript. The data can be found in the graphs, the models in the equations.